

Heat Transfer / Film Cooling

Paper 26

**ON TESTING THE AERODYNAMICS OF
FILM-COOLED BLADES**

V. Dossena, C. Osnaghi (Politecnico di Milano, Italy)

A. Perdichizzi, M. Savini (Università degli Studi di Bergamo, Italy)

ON TESTING THE AERODYNAMICS OF FILM - COOLED BLADES

V. Dossena*, C. Osnaghi*

A. Perdichizzi**, M. Savini**

*Dipartimento di Energetica, Politecnico di Milano, Piazza Leonardo da Vinci 32, 20133 Milano, Italy

**Facoltà di Ingegneria, Università degli Studi di Bergamo, Viale Marconi 5, 24044 Dalmine (Bg), Italy

Abstract

The paper presents the details of the measuring techniques developed for testing film-cooled blades. Two different topics are here addressed; the first one concerns the testing procedures used to characterize the aerodynamic behaviour of a full-coverage film cooled gas turbine nozzle. The main points focused include the measurements of discharge coefficients of the rows of holes, the use of air and CO₂ as coolant flow completed with a critical comparison of the loss evaluation. An approximate method for the data reduction in case of difference in the nature of coolant and main flow is also provided.

The second point concerns the accomplishment of a fully automated system to perform a 3D map of the flow field downstream of a cascade in order to study the wake development and the mixing process occurring in this region. A post-processing method for measurements in regions of high gradients, i.e. in the near wake, is here also presented

Nomenclature

c_p = specific heat at constant pressure
 C = concentration
 C_D = discharge coefficient
 d = diameter
 h = height
 I = momentum flux ratio (jet to freestream)
 m = mass flow rate
 M = Mach number
 MFR = mass flow ratio (jet to freestream)
 P = pressure
 R = gas constant
 Re = Reynolds number
 s = pitch
 T = temperature
 V = velocity
 x, y, z = axial, pitchwise, spanwise coordinate
 β = flow angle (from tangential direction)
 γ = specific heat ratio

ζ = energy loss coefficient

ρ = density

Subscripts

1 = inlet
2 = exit
 c = coolant
 d = design
 ext = external
 is = isentropic
 mix = mixture
 pr = primary
 Ref = reference, i.e. design
 s = static
 th = thermodynamic
 T = total

Introduction

Full coverage of turbine blades by film cooling is commonly employed in the first stages of modern gas turbine engine design. In fact film cooling results as the best mean to sustain higher inlet temperatures in order to improve the overall efficiency of the engine cycle.

The injection of the coolant produces two different effects: the first one is the reduction of the blade wall temperature; the second one is the aerodynamic mixing between coolant and mainstream, the latter producing losses that may reduce the expected turbine efficiency.

In the last years, many analytical and experimental studies have been carried out in order to compute the effects of air cooling on the aerodynamic performances of the bladings [1,2,3,4], but the open literature presents a relative lack of data regarding loss penalties associated with full coverage film cooled blade. To enhance the comprehension of the phenomena and to supply a set of data, a wide experimental research programme has been undertaken at the C.N.P.M.(Centro Nazionale per la Propulsione e l'Energetica, Milano) laboratories wind tunnel. The experiments are focused on the analysis of the 3D mixing process downstream of a full coverage film cooled blade cascade.

The purpose of this paper is to present the experimental technique developed for the above mentioned research; putting more emphasis into the details of the experimental set-up, data reduction and loss evaluation technique, rather than to the results of the research.

The first problem encountered in testing film cooled bladings, consisted in establishing test conditions as close as possible to the real engine conditions. Matching the experimental conditions to the real engine values is very difficult. As well known, it is impossible to reach the same temperature conditions, and a compromise is certainly needed.

One of the most important parameters governing the interaction between mainstream and coolant is their density ratio; to approach design condition, a common practice consists in injecting carbon dioxide as coolant. To this aim, tests has been performed both with air and CO₂ in order to clarify and compare the differences in the two cases. Therefore, particular attention has been given to the data reduction and loss evaluation, to account for the variations of fluid thermodynamic properties, particularly in case of CO₂ injection.

In studying the effects connected to the aerodynamic interaction of the coolant flow with the mainstream flow, it is very important to describe the evolution of the mixing process downstream of the cascade. Therefore, a fully 3D traversing system (both for 5-hole miniaturized pressure probe and for hot wire probes) was set up, allowing for a continuous acquisition of the flow characteristics in a 3D control volume downstream of the linear cascade. By means of the application of this traversing system, it is possible to analyse the development of the mixing process in a single test run.

Experimental apparatus

Wind Tunnel

The tests were performed at the CNPM laboratories wind tunnel. The tunnel is a blow down type facility, with a test section of 380x80 mm and an air storage capacity of 3100 Kg at 200 bar, permitting relatively long running times also in transonic or supersonic conditions.

In order to perform tests on cooled blades, the tunnel has been modified and the fundamental features of the actual experimental set-up are reported in Fig. 1:

- The main flow feeding system is equipped with a diathermic oil heater to make possible tests with a significant temperature difference (50-80 °C) between main and secondary fluid.
- To provide a high turbulence level at the cascade inlet, a turbulent generator has been installed. After several tests with different geometries [5], the actual turbulence generator consists in a row of bars of diameter $d = 5$ mm and pitch to diameter ratio of 2, located at an upstream adimensional distance of $x/d = 37$. The device provides a turbulence level at the cascade inlet of $Tu \cong 6-7$ %, approaching the one existing in the real engine.

The turbulence level Tu is defined as $Tu = \sqrt{\frac{2}{3} \frac{k}{\bar{V}^2}}$, where k is the turbulent kinetic energy, and \bar{V} the freestream velocity. The various tests showed that Tu decays rapidly with the distance from the bars. This behaviour is approximated by the empirical relation:

$$Tu = 57.3 \left(\frac{Re}{10^5} \right)^{-0.25} \left(\frac{x}{d} \right)^{-\frac{5}{7}}$$

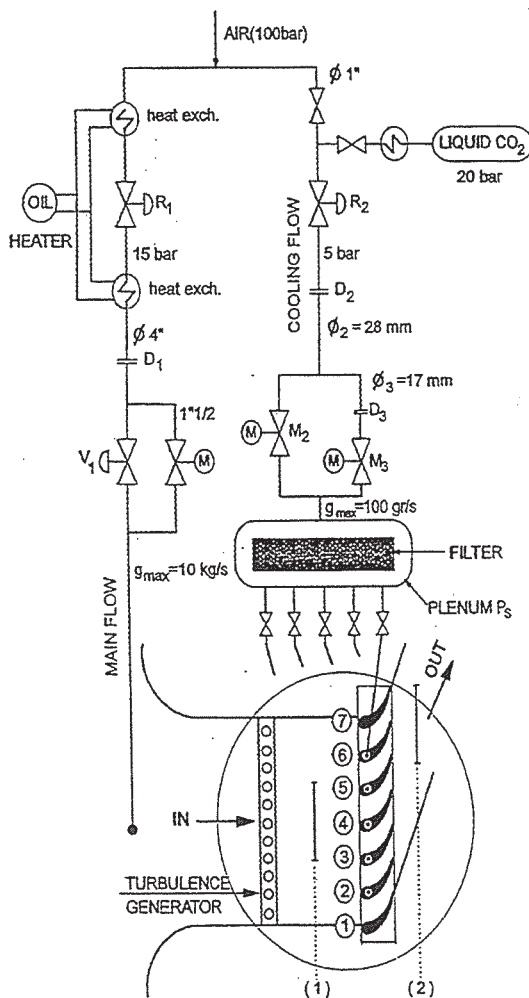


Fig. 1: Lay out of test rig

- The secondary flow feeding system can supply both air or carbon dioxide. The CO₂ is supplied by a tank at 20 bar, where it is stored in liquid phase. The piping line is equipped with a pressure reduction valve, a heat exchanger to assure complete vaporization, two motorized valves for the mass flow rate regulation, and a filtering section located in the plenum that feeds the cooled blades. The coolant mass flow rate is measured by means of two instrumented orifices (D2 and D3 in Fig. 1) of different diameters, in order to cover flow rates ranging from 0.005 to 0.1 kg/s. The set of orifices (4 to 15 mm diameter) have been calibrated by means of efficient and miniaturized sonic nozzles.

Cascade Geometry

The tested vane geometry is qualitatively reported in Fig.2. The cascade consists of 7 blades scaled from a first stage nozzle vane. A unique inner cavity, feeds 11 rows of cylindrical holes distributed along the profile and a row of rectangular holes at the trailing edge of the blade. The blowing geometry, reported qualitatively in Fig. 2, covers approximately 85% of the span.

Since the nominal design velocity is close to the transonic regime, particular attention is required to satisfy the periodicity condition in the downstream flow. To this aim, 5 film cooled blades has been manufactured and located in the central part of the cascade so that 4

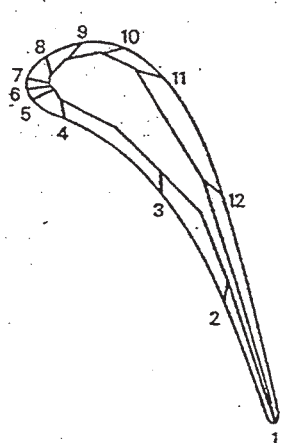


Fig. 2: Film cooled nozzle guide vane

central passages had the same coolant injection. Moreover, a movable tailboard located at the exit of the first blade allows for the adjustments of the sidewall boundary condition.

To get the profile static pressure distribution at midspan, two adjacent blades have been instrumented: one with 15 pressure taps on the pressure side, the other with 19 taps on the suction side.

Testing Procedure

The tests have been carried out by means of a fully automated computer-controlled data acquisition system. To set the tunnel at the desired testing condition, a procedure has been developed performing the real time monitoring of the coolant to mainstream mass flow rate ratio (MFR) and of the outlet isentropic Mach number. The cooling flow rate is measured by an orifice device; the main flow rate is evaluated from the upstream probe data and is based on a reduced blade height to make it consistent with the partial cooling ejection along the span.

The total pressure of the cooling flow is measured in the inner cavity of the vane by a wall pressure tap on the upper plug of the blade, i.e. on the same side of the coolant inlet. A thermocouple fitted on the same plug provides the total temperature of the cooling flow. The flow conditions at the cascade inlet are measured by a wedge-type 3-hole probe located upstream of the leading edge. The downstream measurements have been carried out by traversing the flow by means of a miniaturized 5-hole probe.

The estimated uncertainties of the measured quantities are given in Table 1.

Pitchwise and spanwise position	± 0.1 mm
Flow angle	± 0.2 deg
Stagnation and static pressure	± 0.15 % ($p_t - p_s$)
Mass flow rate	± 1.5 %

Table 1. Experimental uncertainties

Loss evaluation

In testing film cooled blades, it is well known that an important parameter governing the coolant-mainstream flow interaction is the density ratio between the two flows. Also the loss production mechanism is influenced by this parameter, and it is an open question if in fully covered film-cooled blade testing it is necessary to match the real density ratio, in order to get the correct losses. To approach such conditions a common practice is to inject carbon dioxide as coolant fluid, but in this case particular attention has to be paid to the data reduction, to avoid errors in the loss evaluation. In the present investigation tests have been performed both with air and carbon dioxide to clarify the differences in the two cases.

The downstream traverse results may be presented in terms of two different energy loss coefficients:

1. The primary loss ζ_{pr} :

$$\zeta_{pr} = 1 - \frac{V_2^2}{V_{2,is}^2} = \frac{\left(\frac{P_{s2}}{P_{T2}}\right)^{\frac{\gamma-1}{\gamma}} - \left(\frac{P_{s2}}{P_{T1}}\right)^{\frac{\gamma-1}{\gamma}}}{1 - \left(\frac{P_{s2}}{P_{T1}}\right)^{\frac{\gamma-1}{\gamma}}}$$

By this simplified definition, the contribution of the cooling flow energy is neglected; it means that the ideal kinetic energy of the cooling flow is assumed to be equal to the one of the main flow.

2. The Thermodynamic loss ζ_{th} :

$$\zeta_{th} = \frac{m(V_{2,is}^2 - V_2^2) + m_c(V_{c,is}^2 - V_c^2)}{mV_{2,is}^2 + m_c V_{c,is}^2} = 1 - \frac{(1 + m_c / m)V_2^2}{V_{2,is}^2 + (m_c / m)V_{c,is}^2}$$

From this definition it results

$$\zeta_{th} = 1 - \frac{(1 + m_c / m)c_{p,mix} T_{T2mix} \left[1 - \left(\frac{P_{s2}}{P_{T2}}\right)^{\left(\frac{\gamma-1}{\gamma}\right)_{mix}} \right]}{c_{p,air} T_{T1} \left[1 - \left(\frac{P_{s2}}{P_{T2}}\right)^{\left(\frac{\gamma-1}{\gamma}\right)_{air}} \right] + (m_c / m)c_{p,c} T_{Tc} \left[1 - \left(\frac{P_{s2}}{P_{Tc}}\right)^{\left(\frac{\gamma-1}{\gamma}\right)_c} \right]}$$

This definition takes into account the energy actually introduced into the flow field by the injection of the cooling flow; therefore this is the loss coefficient to be considered if one wants to establish the actual energy decay in the whole blade system, including the feeding loss in the cooling holes, the mixing loss due to the injection and the profile loss. Therefore, the thermodynamic loss coefficient ζ_{th} has to be considered as more significant in the results analysis.

Data reduction

To determine ζ_{th} in each point of the measuring grid, the local value of coolant concentration has to be known in order to evaluate the local value of T_{T2mix} . In particular, in case of CO_2 injection, the actual thermodynamic properties, R and γ of the main-flow/coolant mixture in the downstream measuring points have also to be known.

Moreover, for the 5-hole probe data reduction procedure, such data are needed to link the Mach number to the calibration data.

To evaluate these quantities, additional traverses of CO_2 concentration and total temperature should be performed for each test, but this would require such long times that is absolutely incompatible with the blow-down wind tunnel running times. To overcome this problem, a procedure has been introduced in the data reduction, which allows to estimate approximately in each measuring point R , γ and T_{T2mix} . This procedure is based on the

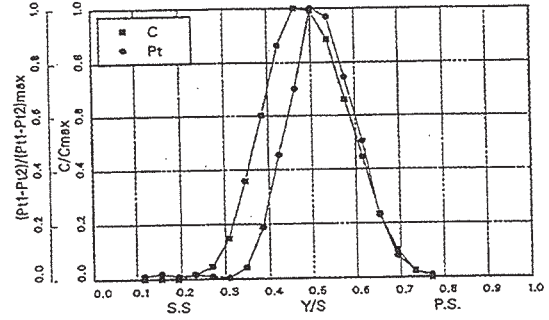


Fig.3 CO_2 concentration and total pressure loss wake

assumption that the distribution of carbon dioxide concentration C along the traverse is consistent with the one of total pressure loss, i.e.

$$\frac{C(y)}{C_{\max}} = \frac{(p_{t1} - p_{t2}(y))}{(p_{t1} - p_{t12})_{\max}}$$

This means to assume an analogy between coolant mass diffusion and momentum diffusion, supposing that the diffusion mechanism is mainly due to the turbulence (Schmidt number $\cong 1$).

The peak value of the coolant concentration C_{\max} is determined in an iterative way, so that the coolant flow rate, obtained by integrating the coolant mass flow rate throughout the passage, is equal to the value measured by the orifice. This procedure can be used not only in the case of CO_2 injection, but also in the case of air injection with total temperature different from the one of the main flow, to estimate the total temperature of the mixture $T_{t2\text{mix}}$. In this case the assumption is that thermal diffusion is mainly due to turbulent mixing (Lewis number $\cong 1$), and that the heat transfer between the coolant and main flow through the blade wall is negligible.

In order to check the validity of the above assumption, the CO_2 concentration for the design injection condition was measured by means of an infrared analyser. The results of Fig. 3 show a larger extent of the concentration wake on the suction side, that is likely to be due to the larger coolant flow rate blown from the suction side, compared to the one from the pressure side.

This result is not in agreement with the assumption made, so a sensitivity analysis was carried out, by considering different concentration distributions (Fig. 4):

- A - Constant distribution along the pitch
- B - Distribution resembling the total pressure distribution along the pitch
- C - Distribution with a higher concentration value in the wake centreline
- D - Same distribution as B, but shifted towards the channel suction side
- E - Same distribution as B, but shifted towards the channel pressure side

The results corresponding to the sensibility analysis are reported in Fig.4 and in Table 2 showing that the local loss coefficient is strictly affected by the assumed distribution, but the pitchwise mass averaged loss variation is not so significant. Table 2 reports the pitchwise mass average loss variation $\Delta\zeta_{\text{th}}$ with respect to the concentration B (corresponding to the above mentioned assumption for the concentration distribution); it is evident that the maximum $\Delta\zeta_{\text{th}} = -0.02 \cdot 10^{-2}$ occurs for the uniform distribution.

On the contrary, Table 2 shows that appreciable variations take place if the overall coolant flow rate calculated from the concentration data does not correspond to the actually injected flow ($\Delta\zeta_{\text{th}} = 0.2\%$ for $\pm 20\%$ error in mass flow rate).

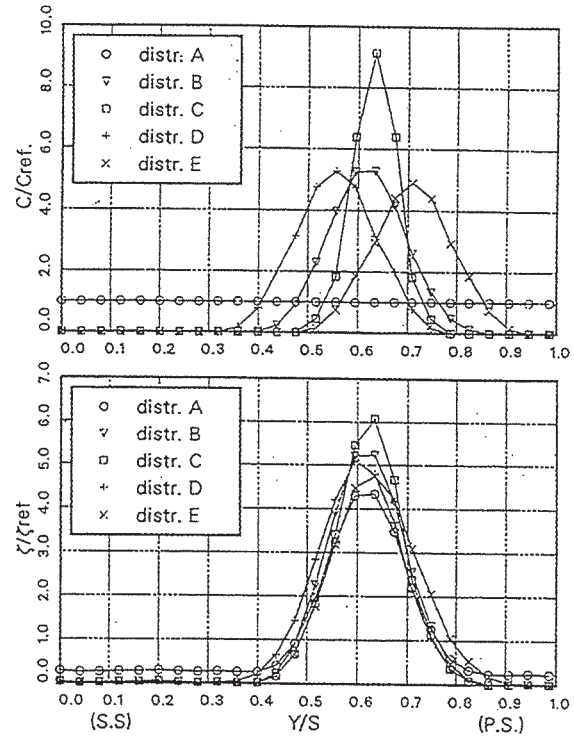


Fig. 4: CO_2 Concentration for the sensitivity analysis and corresponding loss traverse results

	DISTR. A	DISTR. B	DISTR. C	DISTR. D	DISTR. E	$m_c - 20\%$	$m_c + 20\%$
$\Delta\zeta_{th} \%$	-0.02	0.00	0.00	0.01	-0.01	0.20	0.19

Table 2: Variation of thermodynamic loss coefficient ζ_{th}

Discharge Coefficients and Coolant Flow Evaluation

The discharge coefficient, defined as $C_D = \frac{\rho v}{(\rho v)_{is}}$, depends, for a given geometry, on the isentropic Mach number M_{is} and Reynolds number Re_{is} , the latter based on the hole diameter. In order to get a reasonable estimate of the influence of the Reynolds number, a set of preliminary tests were conducted on perforated plates with holes of different diameter. It is very difficult to separate in the experiments the effects of the Mach number and Reynolds number, so we prefer to write the relation obtained via this set of tests in the form:

$$C_D = C_D^*(M_{is})f\left(\frac{Re}{Re^*}\right)$$

where the asterisk refers to a given test condition (d , l/d and kinematic viscosity ν) and is, strictly speaking, $C_D^*(M_{is}, Re^*(M_{is}))$. In the range of interest from incompressible to choked flow, the following function gave the best fit:

$$f = \left(\frac{Re}{Re^*}\right)^{0.04}$$

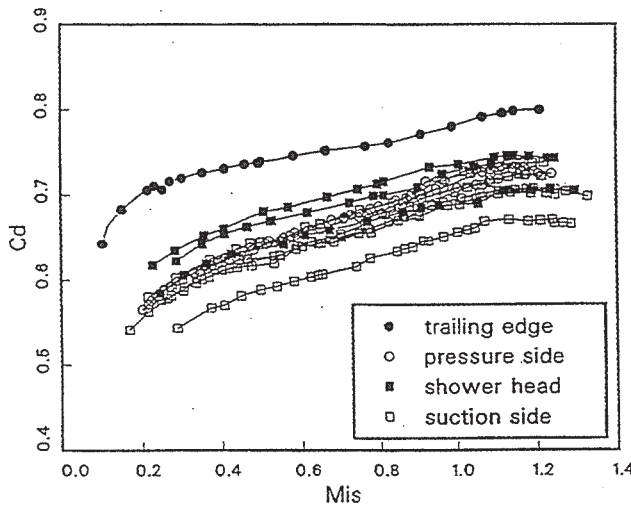


Fig. 5: Discharge coefficients for all rows of holes

By means of this function one can correct the experimental C_D^* data base, in order to take into account the scale effects and the effects of viscosity and density differences between the calibration and the wind tunnel or real gas turbine application. By changing the inner blade pressure, with the outlet pressure fixed (atmospheric), we obtained the curves of Fig. 5 for the 12 rows of holes. The trend of the curves is quite similar and congruent with the l/d ratio, except for the trailing edge holes which have a different shape and an

higher hydraulic diameter. More details can be found in [5].

Owing to the small dimensions involved, great attention was devoted to minimize the leakage and the errors in the evaluation of the hole diameter. A further delicate point was the definition of a reference total pressure, because in the blade cavity the velocity is not negligible, when all the rows of holes are open. In this case a correction was applied to the acquired total pressure value; the correction was determined from tests with no external flow, so that the sum of the coolant rate ejected from all the rows, evaluated by means of the discharge coefficients, corresponds to the coolant mass flow rate measured by the orifice device.

Comparison of losses at different MFR for air and CO₂

Fig.6 and 7 show the trend of traverse averaged losses versus the mass flow rate both for air and CO₂. The values of ζ_{th} , MFR, and I, are made non-dimensional with respect to the design condition.

Fig. 6 shows the losses produced by air and CO₂ reported versus the MFR, i.e. versus the same mass flow rate

Fig. 6 evidences that for small injection rates ($< 0.7 \text{ MFR}_d$), the loss coefficient is not very sensitive to the MFR variation. The remarkable difference of ζ with respect to the value for $\text{MFR} = 0$, is due to the fact that this last data is relative to a solid blade, i.e. same profile but without rows of holes. Therefore we can notice that the ejection rows of holes introduce an additional loss, even at zero blowing rate. This is caused by the superposition of two effects: one is the well-known fact, e.g. Ito et al. [7] and Arts [1], that the presence of the holes may both trigger the transition of the boundary layer and increase the turbulence of a turbulent boundary layer; the other is due to the fraction of the mainstream entering the hollow cavity in the leading edge region and exiting from the suction side and from the trailing edge holes, thus experiencing an additional dissipation. In order to separate these two effects the holes should be sealed from the inside; however, this was not done in the course of the present work.

Increasing the blowing rate, the loss increases significantly, with a higher rate for the case of air injection. This is mainly due to the higher velocity required for the air injection at the same mass flow ratio. In fact higher velocities cause higher dissipation inside the internal passages. This is clearly shown in Fig.6 where global losses are compared to external losses, calculated as global minus internal losses. The last were computed by mass averaging the internal loss of each single row, being the loss and the sharing of flow rate evaluated on the basis of the discharge coefficients data base.

The difference in air and CO₂ loss coefficients values tends to disappear, if one represents the losses at fixed momentum flux rate instead of MFR. This is done in Fig. 7, comparing the data at fixed MFR for air with the corresponding loss for CO₂ injection at a MFR obtained by multiplying the air MFR for the square root of the density ratio between air and CO₂. Fig. 7 suggests that the most important parameter in the aerodynamic loss generation process is the momentum flux ratio rather than the mass flow ratio. The result is in agreement with the one of Mee [2] obtained for single trailing edge injection. This is surprising because, in the present case, a change in density ratio at constant I implies a change in the share of coolant among the rows. Therefore it is authors' opinion that this result has not to be considered of general validity.

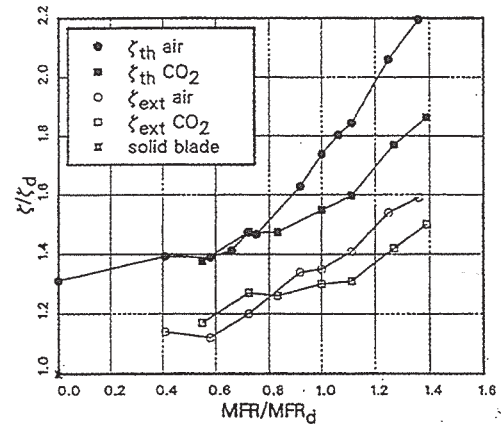


Fig. 6: Global and external losses vs. MFR

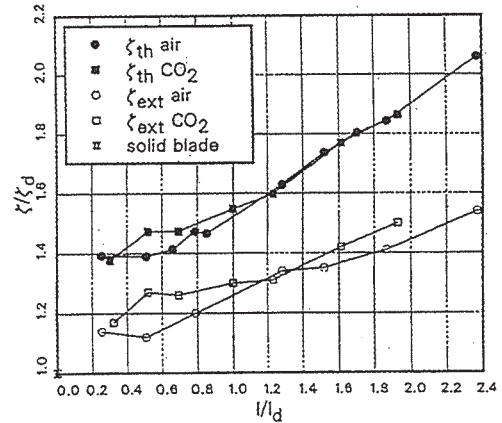


Fig. 7: Global and external losses vs. Momentum Flux

The above described behaviour can be related to the fact that internal losses are in this tests the principal cause of loss increase associated with the coolant injection. In fact, standing the hypothesis of laminar regime inside of the injection holes - so that the friction coefficient inversely proportional to the coolant velocity- and considering only the internal loss, one can conclude that the loss coefficient depends only on the momentum flux ratio. This is in agreement with the low values found for the discharge coefficients (due to the sharp hole inlet and to a probable crossflow inside of the blade cavity) and with very low mixing and cooling-induced boundary layer losses of the actual profile. Moreover the work of Pietrzyk et al. [8] showed that the mixing process, downstream of the injection holes, is dependent on the density ratio, this being more and more important when boundary layer effects becomes dominant.

Therefore we can conclude that it is advisable to perform experiments with a density ratio as close as possible to the actual value of the real engine.

Traversing system for 3D mixing analysis

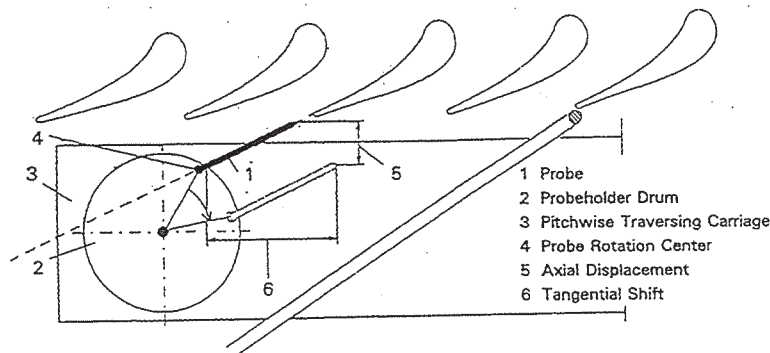


Fig. 8: New traversing system

The use of fully 3D bladings design(end-wall contouring, bowed and leaned blades) with massive application of cooling techniques is a common practice in modern gas turbine design. The aerodynamic testing of such bladings require detailed 3D measurements for the description of the downstream flowfield, being the bi-dimensional analysis

definitively inadequate. To this aim a fully 3D traversing system, which allows for the automatic positioning of the probe (5-hole or hot wire probes) in the points defined by a tridimensional measuring grid, has been developed. The advantage of this system is that a complete 3D flow field may be investigated in a single run.

The original system, designed for the analysis of the flowfield in a secondary plane (i.e. tangential-spanwise direction), has been modified in order to permit a continuous probe displacement also in axial direction. Thus, actually it is possible to define a measuring grid in a blade to blade plane. The combination of the three motion possibilities allows for the definition of the 3D flowfield in a 3D measuring grid downstream of the cascade.

The geometrical constraints of the test-section and the problems involved with the sealing of a linear translator in both axial and tangential directions, drove to a 4 axis system, which allows for the axial displacement of the probe by means of two eccentric rotation centred around parallel axis. The traversing system is reported in Fig. 8: the probe is mounted on a rotating probeholder drum while the probe can also be rotated around its stem.

In order to follow a single streamline along the downstream flow development, in case of 5-hole probe, a tangential shift translation, operated by the pitchwise traversing carriage ,is required. After each axial translation the probe is positioned with the cone axis on a parallel direction corresponding approximately to the mean flow direction, this in order to prevent aerodynamic overloads and to assure the maximum range of yaw and pitch angle definition.

In this way it is possible to define a blade to blade measuring grid, and the stacking of several blade to blade grids, located at different spanwise co-ordinates allows for the definition of the whole measuring volume.

The four probe movements (spanwise, pitchwise and the two rotations) are carried out by means of four stepping motors, controlled by feedback provided by four encoders.

The control software requires as input data the geometrical characteristics of the test section, cascade geometry, probe dimension and measuring grid definition. After a preliminary control about the feasibility of the movements required to reach all the measuring points, the software provides for the following operations:

1. Probe positioning: before each movement of the probe, the software analyses and chooses the best sequence of movements to reach the next measuring point, in order to prevent damages of the probe caused by interaction with the physical borders of the test section.
2. Data acquisition: in each measuring point the software provides for the acquisition of the following quantities:

- pressure data from downstream 5-hole probe
- 3 pressure data from upstream probe
- Total temperature of the main flow
- 4 encoders value from the four motors
- coolant total temperature and pressure inside of the blade chamber
- coolant mass flow rate

3. Display monitoring of the probe movements and test parameter

- Isentropic Mach number
- Blowing rate
- Main and coolant flow parameters (i.e. Total temperature and pressure)

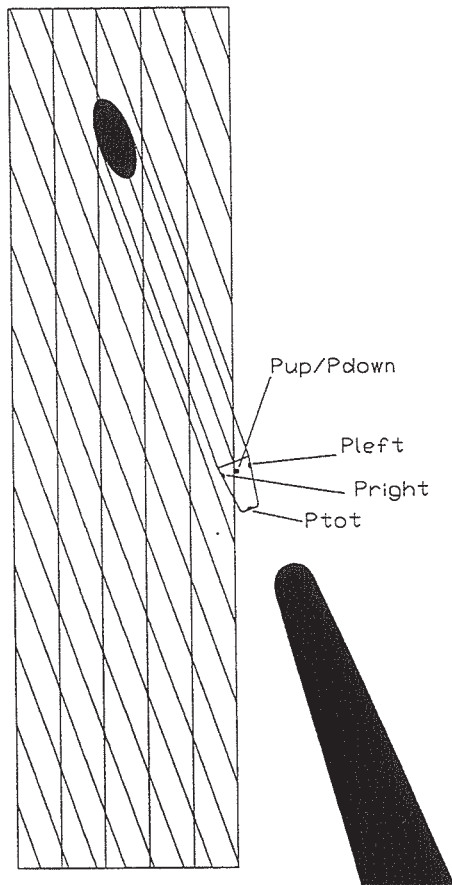


Fig. 9: 5-hole probe and measuring grid

Measurements in high gradients areas

When the 5-hole probe is traversed in areas characterized by high pressure differences over small distances (compared to the probe head diameter), it is no more possible to deduce the 3D flow characteristics simply by means of the calibration data. In fact the probe is calibrated in a uniform flow and it misunderstands the pressure gradient leading to an over-estimation of the yaw angle and to static pressure errors. This implies an error in the calculation of the local flow rate, driving to a consequent error in the mass averaged

loss computation. This happens especially in wake traversing, in particular when the measuring point is located at a small downstream distance with respect to the trailing edge thickness (base region). This problem was already dealt with in a previous paper, but now a new technique has been developed leading to an easy and more reliable data reduction in such areas.

The method is based on a numerical 2D interpolation of the data provided by the 5-hole probe. The pressure taps affected by the blade to blade gradients (usually the most significant ones) are the yaw (left and right) and the total pressure ones.

The first step is to associate each pressure data to the two physical coordinates corresponding to each one of the three involved pressure taps, obtaining three different grids at which nodes are respectively associated the left, right and total pressure values. The second step consists in evaluating the values of the three pressure data in the same physical points of the measuring grid, corresponding to the up/down taps position. By means of a bi-linear interpolating routine it is possible to deduce the values corresponding to each point of the blade to blade plane. In this way, the 5 pressure values, originally acquired in different positions, are reduced to a single physical point and they are used as inputs to get the three velocity components by the standard routine based on the probe calibration coefficients.

Fig. 10 allows for the comparison of the pitchwise distribution of the local outlet angle β , loss coefficient ζ and Mach number, obtained by the application of both standard and new data reduction techniques to blades scaled from a high pressure first stage nozzle of a steam turbine. The results are reported along three pitchwise traverses located at a different axial position, for an isentropic downstream Mach number of 0.85.

The first traverse, located 2 mm downstream of the trailing edge, shows a more uniform Mach number and outlet angle distribution when using the new technique. In particular, the two angle distributions put to evidence an over-estimation of the outlet angle across the wake in standard mode. This can be related to the presence of streamwise gradients in this region. In fact, notice that traversing is made in the pitchwise direction, and not in the normal direction, where pressure gradients are usually negligible.

The local distribution of ζ does not appear to be significantly influenced by the new data

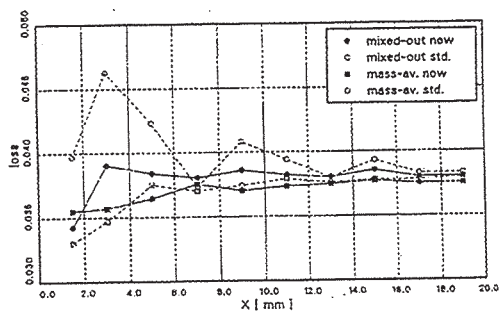


Fig. 11: Mixed out and mass average losses downstream. Standard and new method

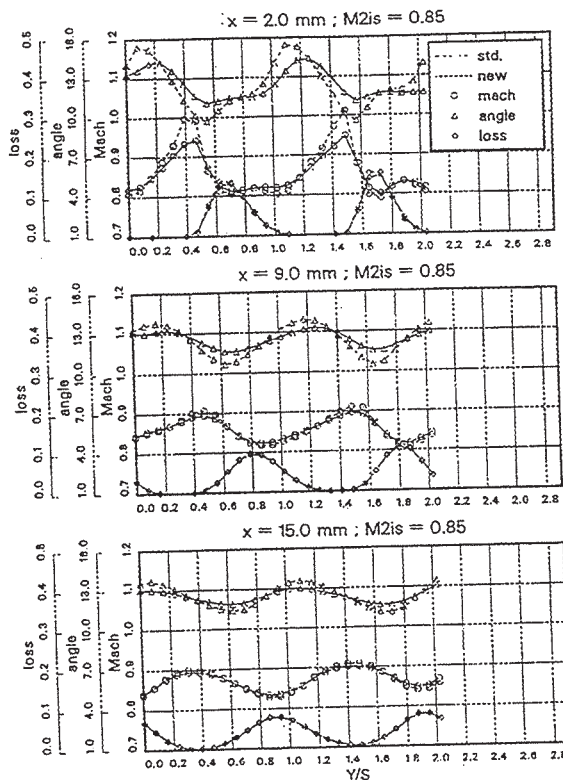


Fig. 10: Mach number, outlet angle and loss coefficient traverse. Standard and new method.

reduction technique. On the contrary the pitchwise mass averaged loss coefficient ζ_{med} is strongly influenced, as shown in fig 11. The first data in Fig. 11, for $x=1.5$ mm, shows a mixed out loss value lower than the corresponding mass averaged one; this evident misleading can be related to an insufficient grid resolution. In conclusion the new method improves the data quality especially in the traverses closest to the trailing edge. This is confirmed by the rapid and progressive increase of

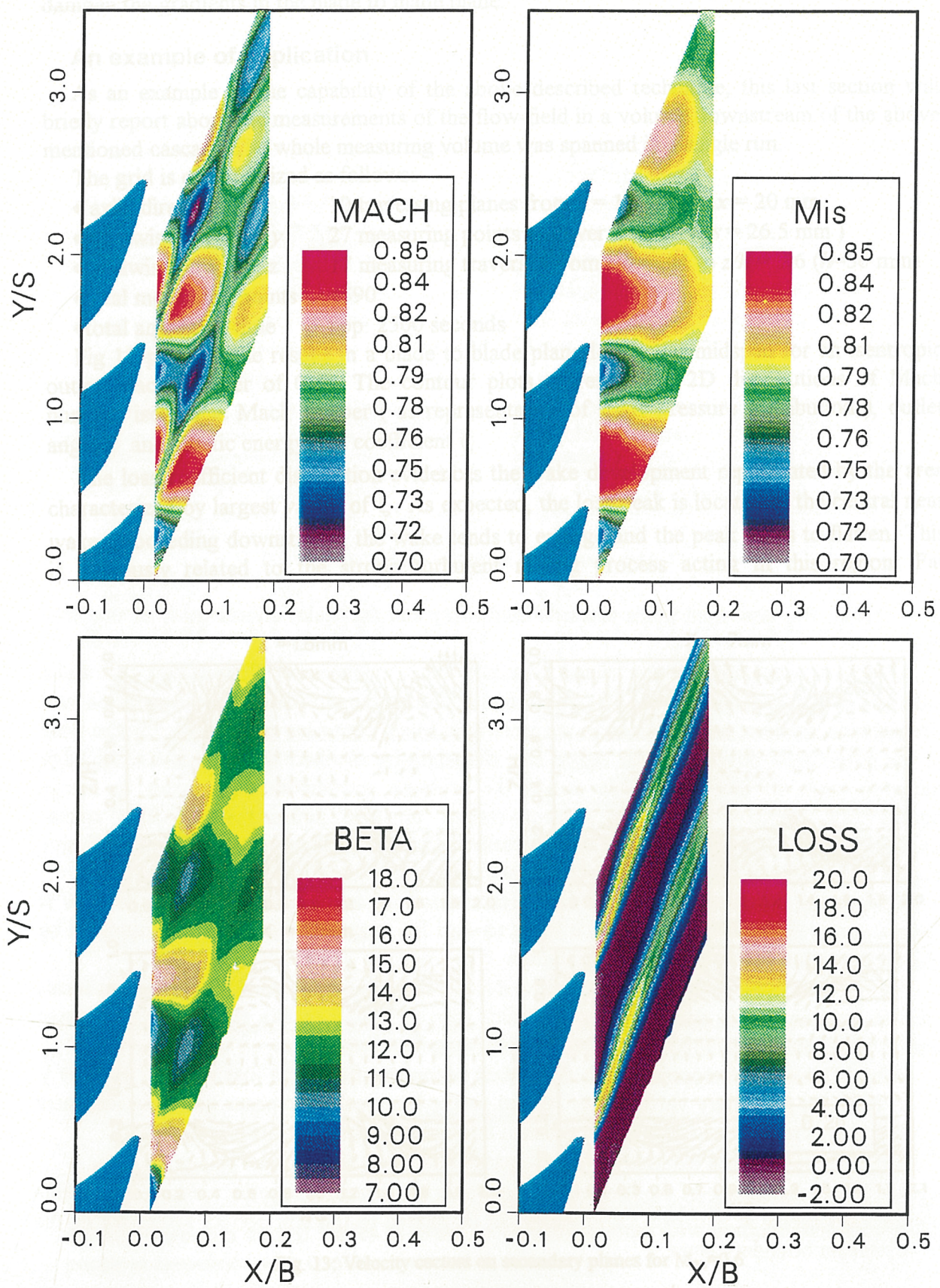


Fig. 12: Mach number, Isentropic Mach number, outlet angle and loss contours on a blade to blade plane for $M_{2is} = 0.85$

the mass averaged loss getting closer and closer to the constant mixed out value.

Proceeding downstream, the differences between the two data reduction techniques, tend to disappear, according to the development of the mixing process that acts in order to dampen the gradients in the blade to blade plane.

An example of application

As an example of the capability of the above described technique, this last section will briefly report about the measurements of the flow-field in a volume downstream of the above mentioned cascade. The whole measuring volume was spanned in a single run.

The grid is characterized as follows:

- axial direction x 10 traversing planes from $x = 1.5$ mm to $x = 20$ mm
- pitchwise direction y 27 measuring points to cover 2 pitches ($s = 26.5$ mm)
- spanwise direction z 17 measuring traverses from $z/h = .04$ to $z/h = .96$ ($h=50$ mm)
- total measuring points 4590
- total acquisition time app. 2500 seconds

Fig 12 presents the results in a blade to blade plane located at midspan for an isentropic outlet Mach number of 0.85. The contour plots represent the 2D distributions of Mach number, isentropic Mach number (as representative of static pressure distribution), outlet angle β and kinetic energy loss coefficient ζ .

The loss coefficient distribution evidences the wake development represented by the area characterized by largest values of ζ . As expected, the loss peak is located in the central near wake; proceeding downstream, the wake tends to enlarge and the peak tends to flatten. This is obviously related to the strong turbulent mixing process acting in this region. Far

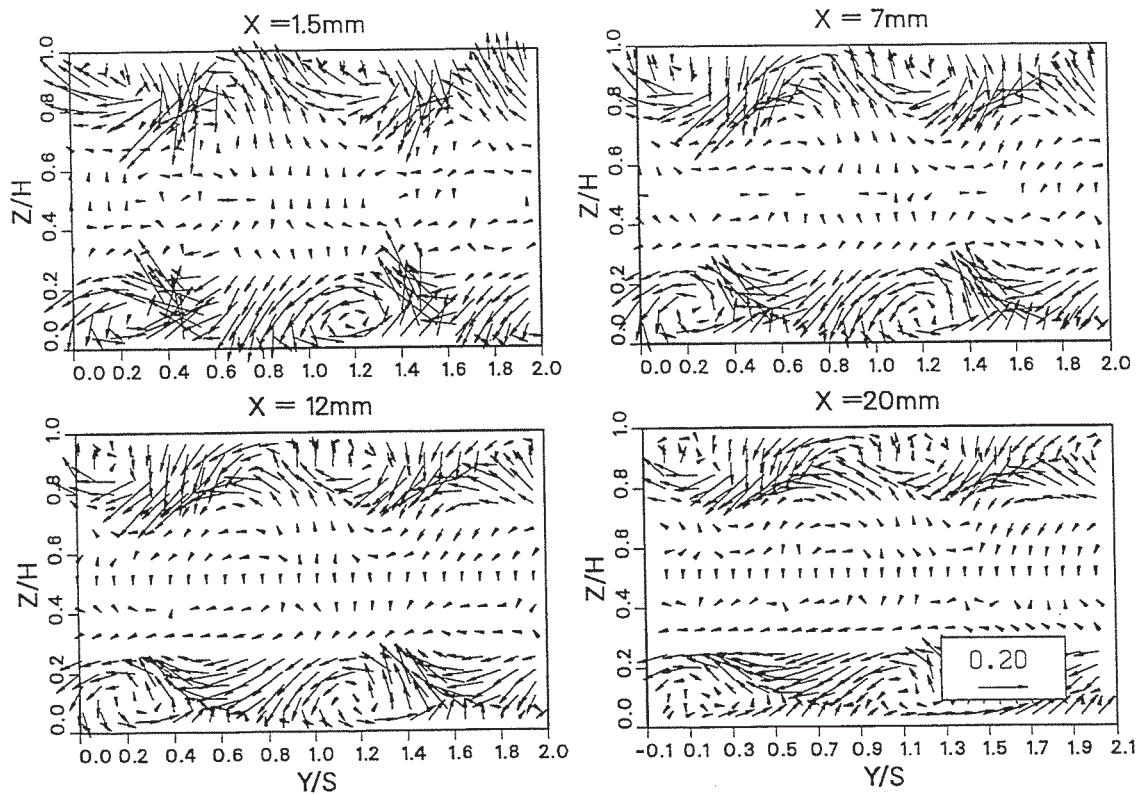


Fig. 13: Velocity vectors on secondary planes for $M_{2is}=0.6$

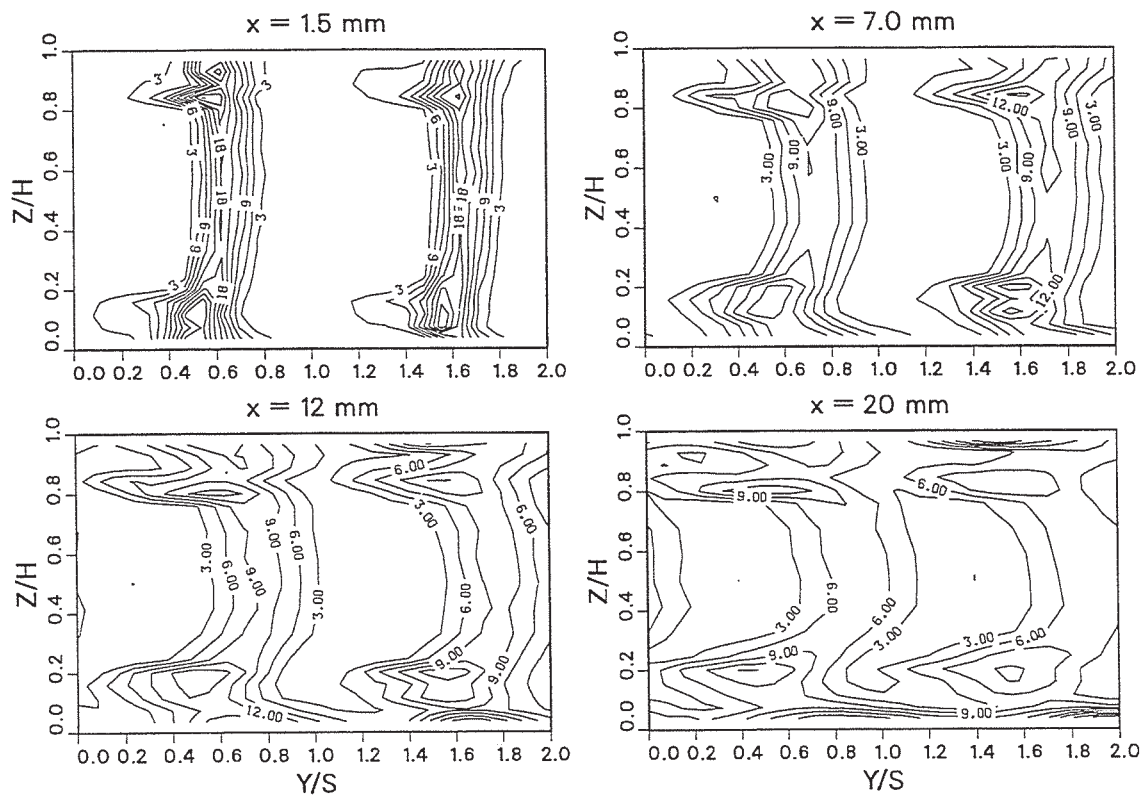


Fig. 14: Loss contours on secondary planes for $M_{2is} = 0.6$

downstream the flow field tends towards uniformity and the wake affects most of the flow field.

At the cascade outlet, the Mach contours bear evidence of a sequence of wake enlargements and contractions. This behaviour is due to the alternating of acceleration and deceleration regions, well depicted in the isentropic Mach contours, encountered by the flow in the streamwise direction; their origin can ultimately be ascribed to the high trailing edge included angle of the blade. This causes the pressure and suction side flows to merge conflictually, thereby generating a cross-stream pressure non-uniformity. The spatial oscillating behaviour continues well downstream and will be finally put to end by the diffusive action of turbulence. The flow angle undergoes to the same trend; when the flow is locally

accelerating (thinning the wake), it turns toward the axial direction, when the flow is decelerating (thickening the wake), it turns toward the tangential direction, as requested by the conservation of the tangential momentum.

Fig. 13 and 14 show the secondary flow development downstream of the profile in terms of loss contours plots and secondary velocity vectors. These results refer to an isentropic outlet Mach number of 0.6, evidencing the following flow features:

- The 3D wake development with the typical secondary flow high loss region (Fig. 14). The strong secondary vortex core, related to the loss peak, decreases going downstream and moves toward midspan whilst the area affected by the vortex becomes bigger
- The 2D flow region extends for a large part of the blade height in all planes.
- A good periodicity of the flow along the whole blade height, together with an acceptable flow symmetry at midspan. Differences can be related to the non perfect symmetry of the upstream boundary layer.

- The typical vortex structure showing passage, shed and corner vortex (Fig.13).
- The secondary energy associated to the vortices, decays rapidly moving downstream..

In figure 15 is shown the static pressure variation in a series of secondary planes during a test at $M_{2is} = 0.6$. The pressure differences in pitchwise direction are related to the above mentioned cross-stream non uniformity in the blade to blade plane and waken progressively downstream. On the contrary, the spanwise pressure differences persist even far downstream and are due to the blockage effect caused by the stem of the 5-hole probe when it is more and more introduced into the flow. What then happens basically is that one is comparing on the same graphs different blade to blade flows, each obtained with a different expansion ratio. If the flow regime is such that there is a relevant variation of the loss and/or flow angle (the most important outcomes of the experiment) with the isentropic Mach number, errors arise when integrating on secondary planes to get mixed out or mass averaged quantities. Anyway, errors are always introduced in the area averaging process whenever 3D effects are relevant so to affect the spanwise distribution of the flow variables. In fact, different expansion ratios drive to different weights (i.e. mass flow rates) in the local terms of the averaging process.

This phenomena become more and more significant as the Mach number increases and the only way to reduce them is to limit the probe stem dimension.

In conclusion, great attention has to be devoted to analyse the static pressure field while performing 3D investigations, especially when approaching the transonic regime.

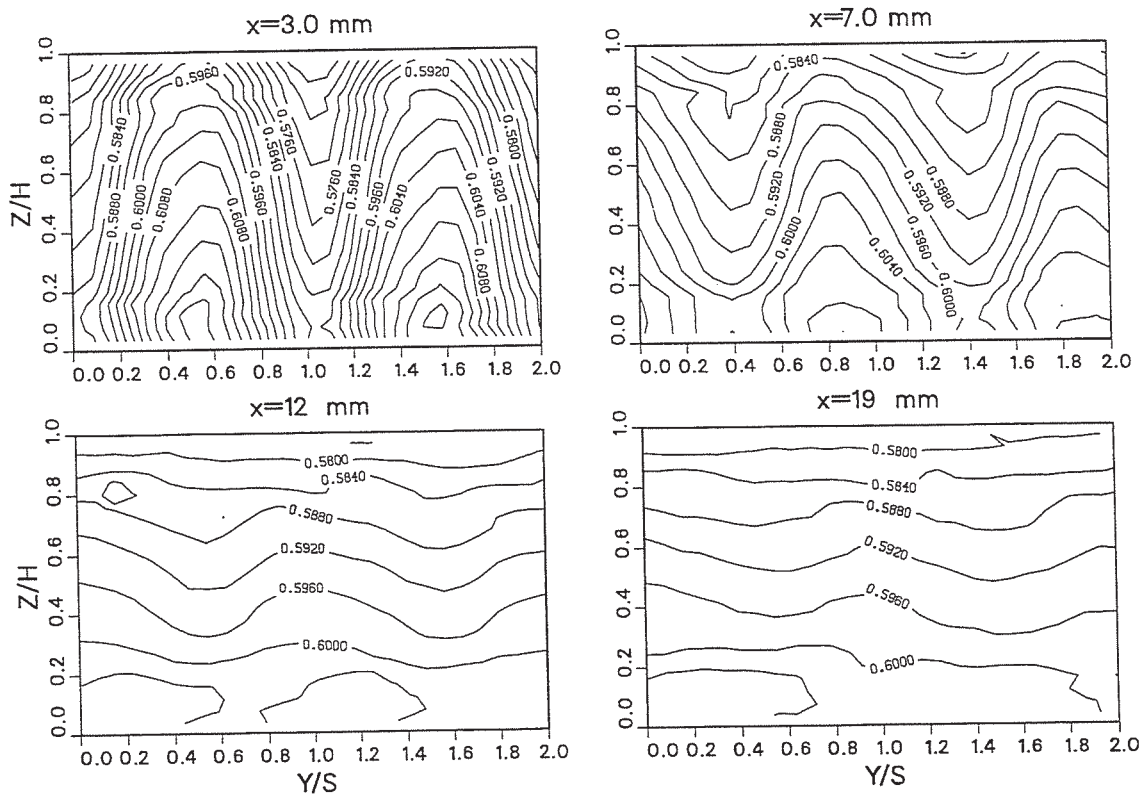


Fig. 15: Isentropic Mach number contours on secondary planes for $M_{2is} = 0.6$

Conclusions

The paper presented the details of a measuring technique applied to 3D investigation of full coverage film cooled blades in order to determine local flow features and aerodynamic penalties associated with coolant injection.

A detailed description of the experimental apparatus has been reported, including turbulence generator test results and the method used for the definition of the discharge coefficients for the rows of injection holes.

Both air and CO₂ have been used as coolant flow, so to simulate different density ratios between main and coolant flow. The thermodynamic loss coefficient was evaluated by means of an iterative procedure based on the estimation of coolant concentration and total temperature.

The loss, both for air and CO₂, have been compared at equal mass flow rates and at equal momentum flux ratio. By referring to the same momentum flux ratio, similar loss levels, have been obtained for the two fluids. This indicates that the most significant parameter to be used in testing film cooled blades, is the momentum flux ratio. However, this is not a result of general validity, as local modifications, depending on different density ratios, take place in the injection regions.

The paper also presented a new fully 3D traversing system for the definition of the flow field within a measuring volume downstream of a linear cascade. The method has been implemented for the detailed description of the development of the 3D mixing process. As an example, the evolution of the flow field in a blade to blade plane and in several secondary planes was also reported.

The paper includes the description of a post-processing technique for 5-hole probes data in order to get more reliable measurements of the flow field in areas characterized by high gradients, i.e. in the near wake region. The capability of the technique is also presented and discussed.

Finally it was pointed out that, even using miniaturized probes, great attention must be devoted to the induced blockage effect.

References

- [1] Kost, F.H., Holmes, A.T.: "Aerodynamic Effect of Coolant Ejection in the Rear Part of Transonic Rotor Blades", AGARD CP 390 "Heat transfer and cooling in gas turbines", Bergen, Norway, May 1985.
- [2] Mee, D.J.: "Techniques for Aerodynamic Loss Measurements of Transonic Turbine Cascade with Trailing-Edge Region Coolant Ejection", ASME paper 92-GT-157
- [3] Yamamoto, A., et al.: "Cooling Air Injection into Secondary Flows and Loss Field Within a Linear Turbine Cascade", AASME paper 90-Gt-141
- [4] Haller, B.R., Camus, J.J.: "Aerodynamic Loss Penalty Produced by Film-Cooling Transonic Turbine Blades", ASME Journal of Engineering for Gas Turbines and Power, Vol.106, pp.198-205.
- [5] Osnaghi, C., Perdichizzi, A., Savini, M., Harasgama, P., Lutum, E.: "The Influence of Film-Cooling on the Aerodynamic Performance of a Turbine Nozzle Guide Vane", submitted for the 1997, ASME-IGTI Gas Turbine Conference.
- [6] Arts, T., Lapidus, I., "Thermal Effects of a Coolant Film along the Suction Side of a High Pressure Turbine Nozzle Guide Vane", AGARD CP 527 "Heat Transfer and Cooling in Gas Turbines", Antalya (Turkey), September 1992.
- [7] S., Eckert, E.R., Goldstein, R.J.: "Aerodynamic Loss in a Gas Turbine Stage with Film-Cooling", ASME Journal of Engineering for Power, Vol.102, pp.964-970.
- [8] Pietrzyk, J.R., Bogard, D.G., Crawford, M.E., 1990, "Effects of Density Ratio on the Hydrodynamics of Film-Cooling", ASME Journal of Turbomachinery, Vol.112, pp. 437-443.